ELSEVIER

Journal of Molecular Catalysis A: Chemical 169 (2001) 207–223

JOURNAL OF MOLECULAR CATALYSIS A: CHEMICAL

www.elsevier.com/locate/molcata

# Characterization of $La_2O_3$-$TiO_2$ and $V_2O_5$/$La_2O_3$-$TiO_2$ catalysts and their activity for synthesis of 2,6-dimethylphenol

Benjaram M. Reddy*, Ibram Ganesh

*Inorganic and Physical Chemistry Division, Indian Institute of Chemical Technology, Hyderabad 500 007, India*

Received 4 August 2000; received in revised form 8 November 2000; accepted 5 December 2000

**Abstract**

The $La_2O_3$-$TiO_2$ (1:5 molar ratio) mixed oxide was prepared by a co-precipitation method with in situ generated ammonia and was impregnated with various amounts of vanadia (4–12 wt.%). The $La_2O_3$-$TiO_2$ and the $V_2O_5$/$La_2O_3$-$TiO_2$ catalysts were subjected to thermal treatments from 773 to 1073 K and were investigated by X-ray diffraction, FT-infrared, BET surface area, and $O_2$ chemisorption methods to establish the effects of vanadia loading and thermal treatments on the surface structure of the dispersed vanadium oxide species and the temperature stability of these catalysts. Conversion of cyclohexanol to cyclohexanone/cyclohexene was investigated as a model reaction to assess the acid–base properties of these materials. The catalytic property was evaluated for a single step synthesis of 2,6-dimethylphenol from cyclohexanone and methanol in the vapor phase at normal atmospheric pressure. Characterization results suggest that the co-precipitated $La_2O_3$-$TiO_2$ when calcined at 773 K is in X-ray amorphous state and exhibits reasonably high specific surface area. The amorphous $La_2O_3$-$TiO_2$ is converted into crystalline compounds $La_2Ti_2O_7$ and $La_4Ti_9O_{24}$ at 873 and 1073 K, respectively. The $La_2O_3$-$TiO_2$ also accommodates a monolayer equivalent of $V_2O_5$ (12 wt.%) in a highly dispersed state on its surface. The $V_2O_5$/$La_2O_3$-$TiO_2$ catalyst is thermally quite stable up to 873 K calcination temperature. When subjected to thermal treatments beyond 873 K, the dispersed vanadium oxide selectively interacts with $La_2O_3$ portion of the mixed oxide and forms a $LaVO_4$ compound. The remaining $TiO_2$ appears in the form of anatase phase. The $La_2O_3$-$TiO_2$ and the $V_2O_5$/$La_2O_3$-$TiO_2$ differ in terms of acid–base properties and the 12% $V_2O_5$/$La_2O_3$-$TiO_2$ catalyst provided a maximum yield of 2,6-dimethylphenol among various catalysts investigated. © 2001 Elsevier Science B.V. All rights reserved.

*Keywords:* Vanadium oxide; $La_2O_3$-$TiO_2$; Mixed oxide; Acid–base properties; Redox properties; Oxygen chemisorption; Dispersion; Thermal stability; 2,6-Dimethylphenol; Cyclohexanol; Methanol

## 1. Introduction

The activity and selectivity of supported vanadia catalysts is known to be very sensitive to the composition of the support and in case of $TiO_2$-supported catalysts, the phase of support [1–3]. Previous research has clearly established that the preferred phase of $TiO_2$ is anatase and that the activity per gram of catalyst increases with increase of vanadia loading up to the point where the surface of the support is covered by a theoretical monolayer of vanadium pentoxide [2–5]. Several methods have been tried in the literature to increase the specific surface area of titania and thermal stability of titania anatase structure [6–9]. These methods include making of nano-composites with a second material such as alumina [10,11]; adding palladium as a stabilizing agent [12]; and doping with cerium [13], silica [14,15], zirconia [16], and tungsten oxide [14]. Recently, we have reported that the titania anatase

* Corresponding author. Fax: +91-40-717-3387.
*E-mail address:* bmreddy@iict.ap.nic.in (B.M. Reddy).

1381-1169/01/$ – see front matter © 2001 Elsevier Science B.V. All rights reserved.
PII: S1381-1169(00)00564-1

structure can be stabilized even up to 1273 K with incorporation of other stable oxides such as $Al_2O_3$, $SiO_2$, and $ZrO_2$ and having vanadium oxide present as a monolayer on these mixed oxide surfaces [10,15,16].

The $La_2O_3$-$TiO_2$ composite material has been employed for various purposes in the literature, such as oxidation of chlorodifluromethane [17], oxidative coupling of methane [18,19], automobile catalytic converter [20], ceramic membrane top layer [21], and adsorbent [22]. Lanthana alone is also an interesting material and has been widely used as a catalyst [23,24] and catalyst support [25], particularly in the oxidative coupling of methane. The lanthanum titanate catalyst activates methane more selectively than the corresponding individual oxides [24]. Thus, $La_2O_3$ and $TiO_2$ have often been utilized as promoters, supports and catalysts; however, the combination of $La_2O_3$-$TiO_2$ containing $V_2O_5$ has not been reported previously.

The aim of the present investigation was to provide basic insights into the structure of $La_2O_3$-$TiO_2$ and $V_2O_5/La_2O_3$–$TiO_2$ catalysts, shedding light on the influence of thermal treatments, oxide loading, and preparation method on both thermal stability and physicochemical characteristics of these materials. In this study, a $La_2O_3$-$TiO_2$ (1:5 molar ratio) binary oxide support was prepared by a co-precipitation method and was impregnated with various amounts of vanadium pentoxide. The prepared samples were then subjected to thermal treatments from 773 to 1073 K in order to understand the temperature stability, dispersion of vanadium oxide, and physicochemical properties of these materials. These effects were monitored by means of XRD, FTIR, BET surface area, and oxygen chemisorption methods. To understand acid–base properties, the conversion of cyclohexanol to cyclohexanone and cyclohexene was investigated. Finally, the catalytic property of these materials was evaluated for a single step synthesis of 2,6-dimethylphenol from methanol and cyclohexanone in the vapor phase at normal atmospheric pressure.

## 2. Experimental methods

### 2.1. Catalyst preparation

The lanthana-titania (1:5 molar ratio) mixed oxide support was prepared by a homogeneous co-precipitation method where ammonia was generated in situ by decomposition of urea at 363 K. [16]. In a typical experiment, the requisite quantities of titanium tetrachloride (Fluka, AR grade) and lanthanum nitrate (Loba, GR grade) were dissolved separately in deionized water, and were mixed together (pH = 2). An excess amount of solid urea with a metal to urea molar ratio of 1:1.5 was also added to this mixture solution. The resulting mixture was heated slowly to 363–368 K on a hot plate with vigorous stirring (pH > 7). Heating was continued at this temperature for six more hours and the pH of the solution was increased to 8.5 by adding dilute ammonia in order to complete the precipitation and to facilitate aging. The resulting precipitate was filtered off, washed several times with deionized water until no chlorides could be detected with $AgNO_3$ in the filtrate. The resulting cake was then oven dried at 383 K for 12 h and finally calcined at 773 K for 6 h in an open-air furnace. Some portions of this calcined support were once again heated at 873, 973, and 1073 K for 6 h in a closed electrical furnace in open-air atmosphere.

The $V_2O_5/La_2O_3$-$TiO_2$ catalyst, containing different amounts of $V_2O_5$ (4–12 wt.%) was prepared by a wet impregnation method. To impregnate vanadia the requisite quantity of ammonium metavanadate (Fluka, AR grade) was dissolved in aqueous oxalic acid solution (2 M). To this clear solution, the finely powdered calcined (773 K) mixed oxide support was added. The excess water was then evaporated on a water-bath and the resulting material was oven dried at 393 K for 12 h and subsequently calcined at 773 K for 6 h under a flow of dry oxygen. The finished catalysts were once again treated at 873, 973 and 1073 K for 6 h in a closed electrical furnace in open-air atmosphere. The rate of heating as well as cooling was always maintained at 10 K per minute.

### 2.2. Catalyst characterization

The X-ray powder diffraction patterns have been recorded on a Siemens D-5000 diffractometer by using Cu Kα radiation source and Scintillation Counter detector. The XRD phases present in the samples were identified with the help of ASTM Powder Data Files. The crystallite size of $TiO_2$ anatase was estimated with the help of Debye–Scherrer equation using the XRD data of the anatase (0 1 0) reflection

[26]. The FTIR spectra were recorded on a Nicolet 740 FTIR spectrometer at ambient conditions, using KBr disks, with a normal resolution of 4 $cm^{-1}$ and averaging 100 spectra. A conventional all glass volumetric high-vacuum (upto $1 \times 10^{-6}$ Torr) system was used for both BET surface area and $O_2$ uptake measurements. The BET surface area was measured by nitrogen physisorption at liquid nitrogen temperature (77 K) by taking 0.162 $nm^2$ as the area of cross section of $N_2$ molecule. Before measurements, the samples were evacuated ($1 \times 10^{-6}$ Torr) at 473 K for 2 h. The $O_2$ uptake measurements were carried out as per the procedure described elsewhere [27].

### 2.3. Catalyst evaluation

The conversion of cyclohexanol and one step synthesis of 2,6-dimethylphenol were investigated in vapor phase under normal atmospheric pressure, in a down flow fixed bed differential micro-reactor, at different temperatures. In a typical experiment ca. 0.5–2.0 g of a catalyst sample was secured between two plugs of Pyrex glass wool inside the glass reactor (Pyrex glass tube i.d. 0.8 cm) and above the catalyst bed filled with glass chips in order to act as preheating zone. The reactor was placed vertically inside a tubular furnace, which can be heated electrically. The reactor temperature was monitored by a thermocouple with its tip located over the catalyst bed and connected to a temperature indicator–controller. The catalyst was heated in a flow of air at 723 K for 5 h, prior to the reaction in order to facilitate activation. After the activation, the temperature was adjusted to the desired temperature and the mixture of methanol and cyclohexanone or cyclohexanol was fed from a motorized syringe pump (Perfusor Secura FT, Germany) into the vaporizer where it was allowed to mix uniformly with air or nitrogen before entering the preheating zone of the reactor. The liquid products collected through spiral condensers in ice cooled freezing traps were analyzed by a gas chromatograph. In the case of synthesis of 2,6-dimethylphenol, the liquid products were quantified by FID with a 10% Carbowax 20 M (length 2 m) column. The main products observed were 2,6-dimethylphenol, 2,6-dimethylcyclohexanone, 2-methylcyclohexanone, 1-methoxycyclohexene and some unidentified products. At higher temperatures, some small amounts of CO and $CO_2$ were also noticed. In case of cyclohexanol conversion, the reaction products were analyzed by FID with OV-17 (length 2m) column. The main products obtained were cyclohexene, cyclohexanone, phenol, CO and $CO_2$ along with some unidentified products. In both cases, the activity data were collected under steady state conditions. The conversion, selectivity, and yield were calculated as per the procedure described elsewhere [28].

## 3. Results and discussion

### 3.1. Thermal effects on XRD phase composition

The BET surface area of $La_2O_3$-$TiO_2$ support calcined at 773 K was found to be 123 $m^2g^{-1}$. The quantity of vanadia required to cover the support surface as a unimolecular layer can be estimated from the area occupied per $VO_{2.5}$ ($10.3 \times 10^4$ $pm^2$) unit of the $V_2O_5$. This theoretical estimation yields a load of 0.145 wt.% per $m^2$ of the support to cover its surface with a compact single lamella of the vanadium pentoxide structure [29]. However, in order to see the influence of vanadia on the thermal stability of the $La_2O_3$-$TiO_2$ support, a range of $V_2O_5$ loadings from 4 to 12 wt.% have been selected in the present investigation.

The X-ray powder diffraction patterns of the $La_2O_3$-$TiO_2$ mixed oxide calcined at various temperatures from 773 to 1073 K are shown in Fig. 1. As can be noted from this figure, the lanthana–titania binary oxide obtained via a homogeneous co-precipitation method and calcined at 773 K is in X-ray amorphous state with broad background diffraction lines due to a poorly crystalline $TiO_2$ anatase phase (JCPDS Files No. 21-1272). With increase in calcination temperature from 773 to 973 K, in addition to an increase in the intensity of lines due to $TiO_2$ anatase phase, presence of a new phase with broad peaks at $d = 2.99$, 2.71 and 3.22 Å can be seen, which are attributed due to the formation of $La_2Ti_2O_7$ (JCPDS Files No. 28–517) compound. On further increase of calcination temperature from 973 to 1073 K, the lines due to $La_2Ti_2O_7$ compound vanished and another group of new broad peaks at $d = 3.36$, 3.28 and 2.54 Å are noted, which are attributed to the presence of $La_4Ti_9O_{24}$ compound (JCPDS Files No. 15–324). Recently, Gopalan and

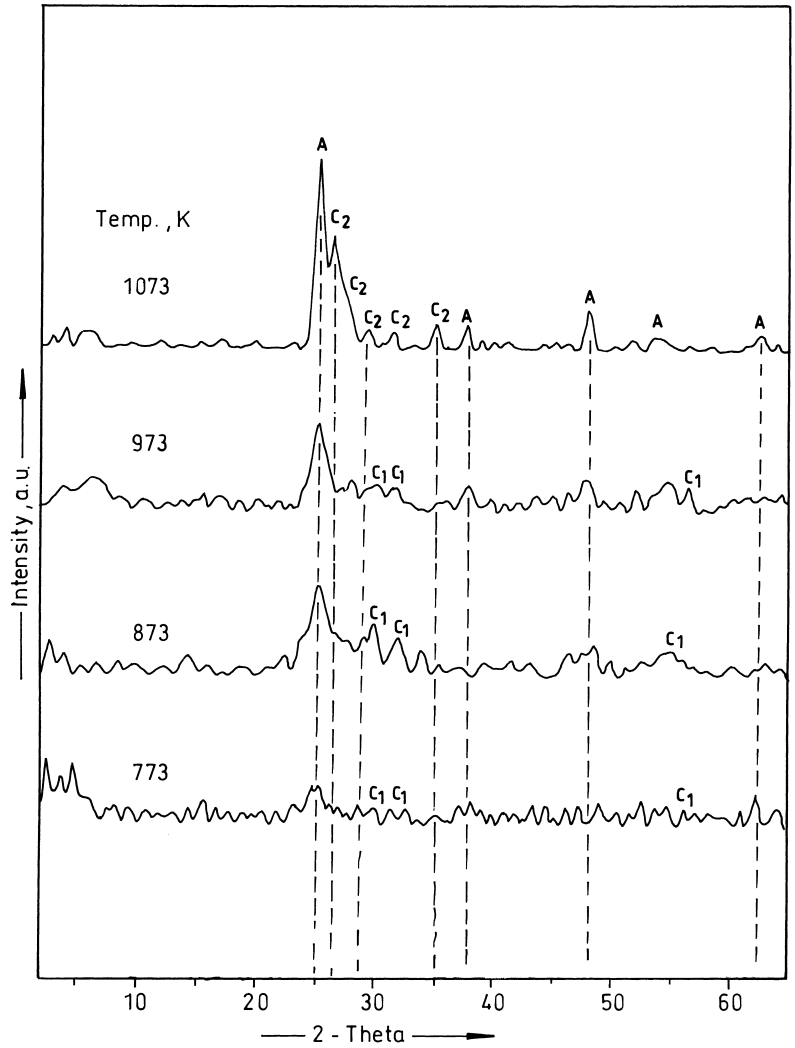


Fig. 1. X-ray diffraction patterns of $La_2O_3$-$TiO_2$ mixed oxide support calcined at different temperatures: (A) lines due to $TiO_2$ anatase; (C1) lines due to $La_2Ti_2O_7$; (C2) lines due to $La_4Ti_9O_{24}$.

Lin [30] also reported the formation of $La_2Ti_2O_7$ compound at 973 K, and $La_4Ti_9O_{24}$ at 1073 K and above temperatures in a sample having the appropriate composition of titania and lanthana components. Very interestingly, no diffraction lines due to $TiO_2$ rutile phase (JCPDS Files No. 21-1276) are observed in the present study even up to the highest calcination of 1073 K. The $La_2O_3$-$TiO_2$ mixed oxide apparently exists in an amorphous phase when calcined at 773 K, and at higher temperatures some portions of this mixed oxide is converted into $La_2Ti_2O_7$ compound and subsequently to $La_4Ti_9O_{24}$, and the latter phase is thermally quite stable up to 1073 K. In a different study, Limar et al. [31] also reported the formation of an amorphous $La_2O_3{\cdot}6TiO_2$, which after dehydration passes into crystalline phases at 973–1073 K as observed in the present study.

The XRD profiles of 4, 8, and 12% $V_2O_5/La_2O_3$-$TiO_2$ catalysts calcined at different temperatures from 773 to 1073 K are shown in Figs. 2–4, respectively. As can be noted from Fig. 2, there are no lines either due to $V_2O_5$ or to a compound between vanadia and

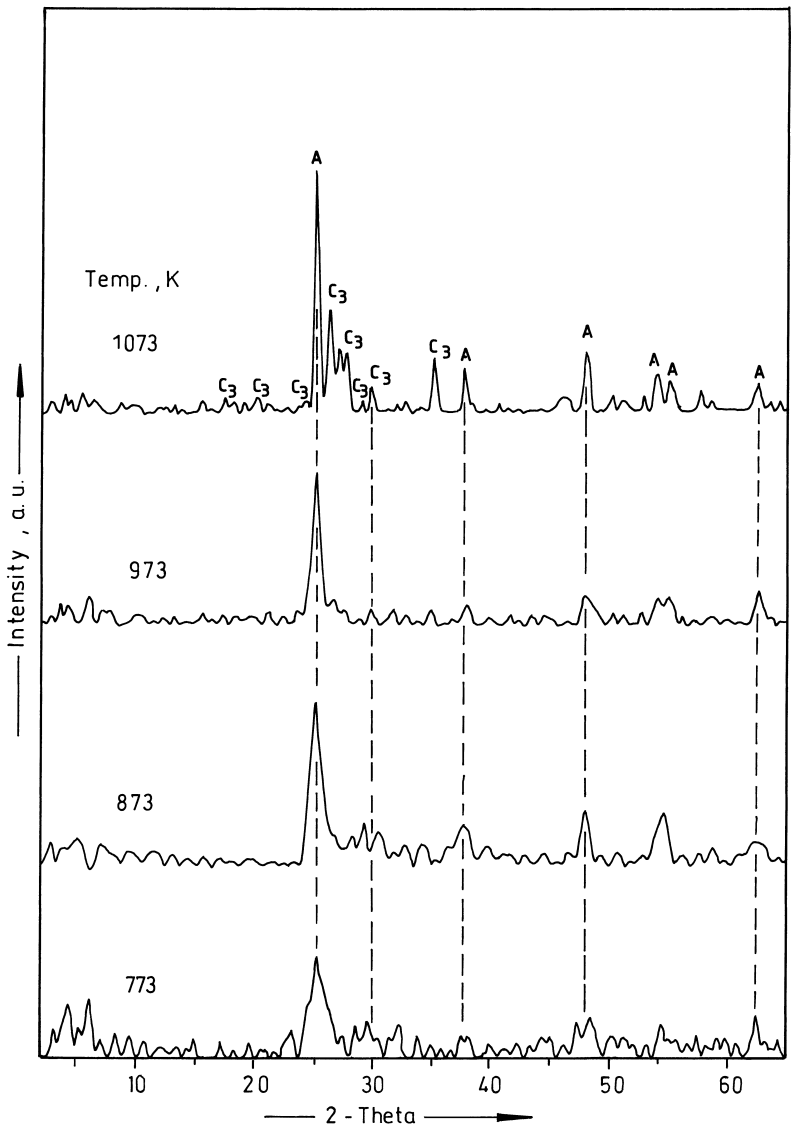


Fig. 2. X-ray diffraction patterns of 4 wt.% $V_2O_5/La_2O_3$-$TiO_2$ catalyst calcined at different temperatures: (C3) lines due to $LaVO_4$; other symbols as in Fig. 1.

lanthana–titania up to a calcination of 973 K, except some broad diffraction lines due to titania anatase phase. The XRD results, thus, indicate that vanadium oxide is present in a highly dispersed state on the mixed oxide support up to 973 K calcination temperature. This observation is further supported from oxygen uptake measurements as described in the later paragraphs. However, at 1073 K calcination temperature in addition to sharp $TiO_2$ anatase lines, some new lines with less intensity were observed at $d = 3.22$, 2.98 and 3.41 Å. These lines can be attributed to the formation of $LaVO_4$ (JCPDS Files No. 25–427) compound. It is well known in the literature that for vanadia contents of less than monolayer coverage the active component will be present as a two-dimensional vanadium oxide over layer on the oxide support. Quantities in excess of monolayer coverage will have microcrystalline $V_2O_5$ particles in addition to the surface

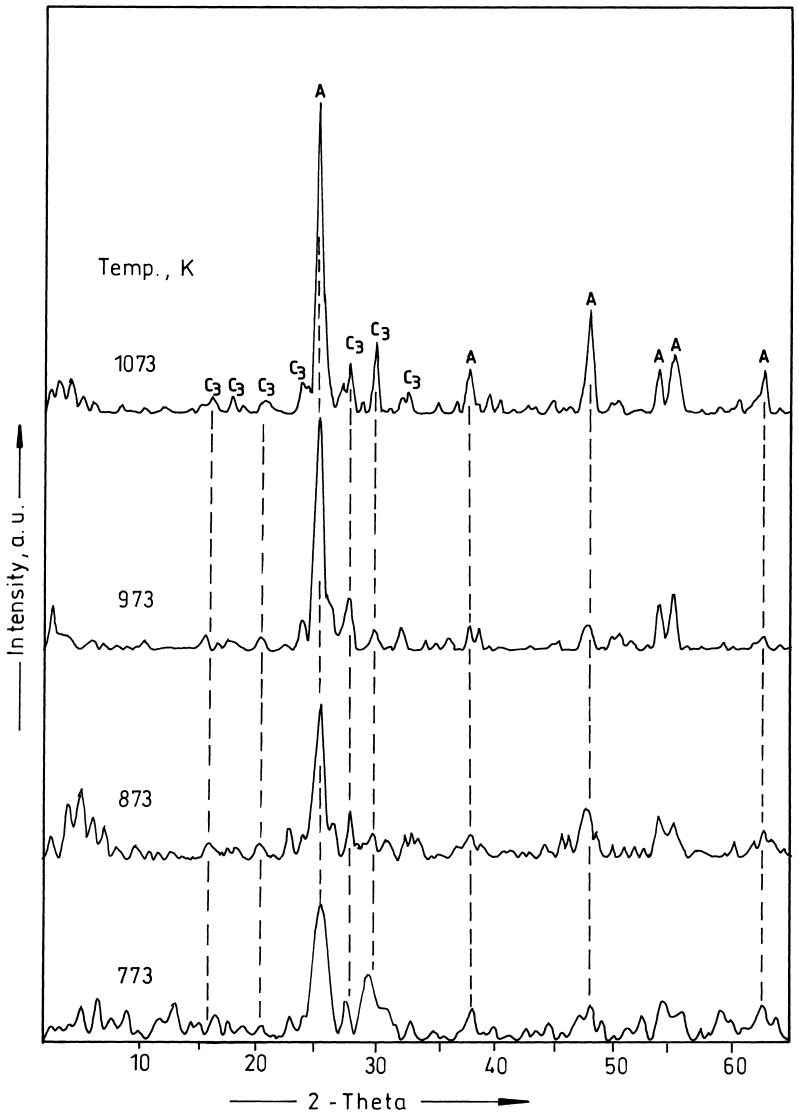


Fig. 3. X-ray diffraction patterns of 8 wt.% $V_2O_5/La_2O_3$-$TiO_2$ catalyst calcined at different temperatures: symbols as in Fig. 2.

vanadium oxide overlayer [2,3]. However, it is interesting to note from Fig. 2 that the formation of $LaVO_4$ compound at 1073 K in the present $V_2O_5/La_2O_3$-$TiO_2$ catalyst system, which is expected to be formed at the expense of dispersed vanadium oxide on the $La_2O_3$-$TiO_2$ surface.

In the case of 8 wt.% $V_2O_5$/ $La_2O_3$-$TiO_2$ catalyst (Fig. 3), the presence of less intense lines due to $LaVO_4$ can be seen at the calcination of 873 K, along with sharp diffraction lines due to titania anatase phase. With increase of calcination temperature from 873 to 1073 K an improvement in the intensity of lines due to both anatase and $LaVO_4$ compound can be noted. In the case of 12 wt.% $V_2O_5/La_2O_3$-$TiO_2$ catalyst (Fig. 4), the intense lines due to $LaVO_4$ compound and $TiO_2$ anatase can be seen even at the calcination of 873 K. On further increase of calcination temperature from 873 to 1073 K, an appreciable improvement in the intensity of lines due to both titania anatase and $LaVO_4$ can be noted.

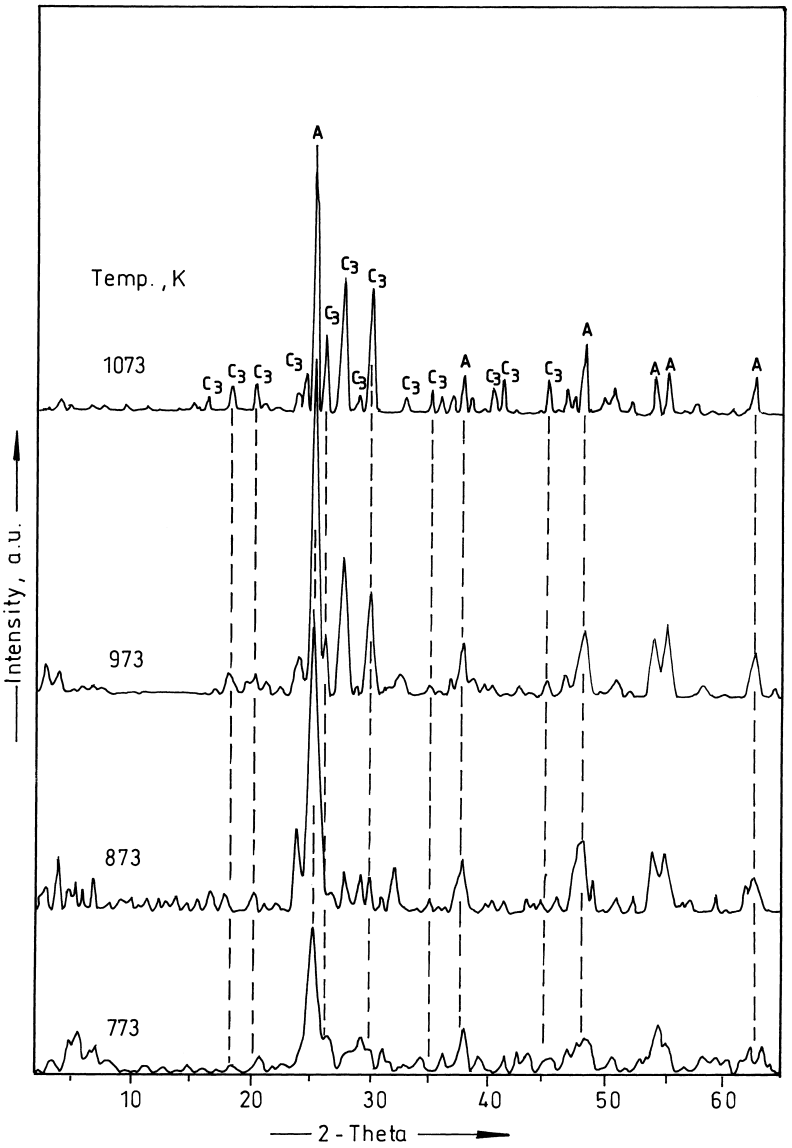


Fig. 4. X-ray diffraction patterns of 12 wt.% $V_2O_5/La_2O_3$-$TiO_2$ catalyst calcined at different temperatures: symbols as in Fig. 2.

From XRD measurements, the crystallite size of anatase phase in various $V_2O_5/La_2O_3$-$TiO_2$ samples was estimated and the results are shown in Fig. 5. As can be noted from Fig. 5 that the impregnated vanadia appears to increase the grain size of anatase in the samples after calcination at higher temperatures. The crystallite size of $TiO_2$ anatase in $V_2O_5/La_2O_3$-$TiO_2$ samples is larger than that of pure lanthana–titania mixed oxide. Increase in vanadia loading also seems to increase the size of $TiO_2$ anatase. These results, thus, suggest that the doped vanadia also accelerate the grain growth of titania. Another interesting point to be mentioned from this figure is the retarding effect of added lanthana on the titania anatase to rutile phase transformation.

A closer examination of Figs. 1–5 reveal that the calcination temperature and presence of vanadia have three major effects on the $La_2O_3$-$TiO_2$ mixed oxide

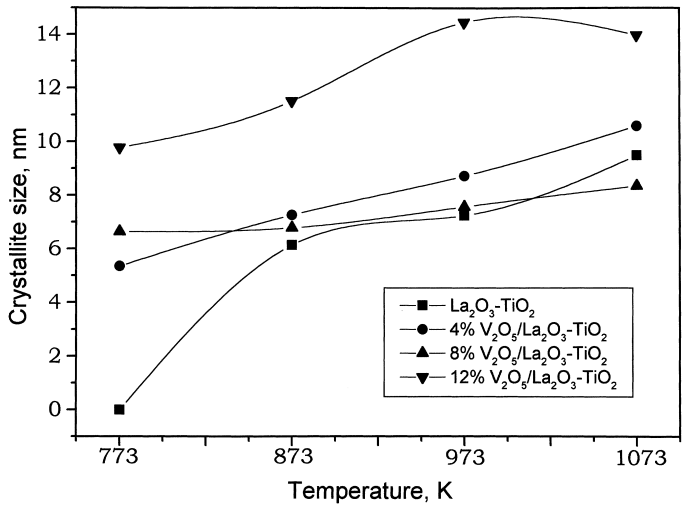


Fig. 5. Effect of calcination temperature on $TiO_2$ anatase crystal growth in various samples. $TiO_2$ anatase (0 1 0) reflection was considered for XRD crystallite size measurements.

support. (a) In the case of pure support, transformation of amorphous $La_2O_3$-$TiO_2$ mixed oxide into definite crystalline compounds $La_2Ti_2O_7$ and $La_4Ti_9O_{24}$ at 873 and 1073 K, respectively. Crystallinity of the remaining titania anatase increases with increase of calcination temperature. The $La_4Ti_9O_{24}$ compound formed at higher temperatures is quite stable in the absence of vanadia. (b) In the case of vanadia containing samples formation of $LaVO_4$ is noted even at 4 wt.% loading (Fig. 2) on increase of calcination temperature from 773 to 1073 K. With increase in the quantity of vanadia, a gradual increase in the intensity of the lines due to $LaVO_4$ and at the same time disappearance of lines due to $La_2Ti_2O_7$ and $La_4Ti_9O_{24}$ compounds can be noted. It can be understood from these figures that the $LaVO_4$ compound is formed at the expense of $La_2Ti_2O_7$ and $La_4Ti_9O_{24}$ phases. Another interesting point to be noted from this figure is that the quantity of vanadia is also an equally important factor in the formation of $LaVO_4$ compound, in addition to the calcination temperature. (c) Absence of a crystalline $V_2O_5$ and appearance of $LaVO_4$ compound accompanied by $TiO_2$ anatase phase for calcination temperatures beyond 773 K was the another important observation. Further, the intensity of lines due to both $LaVO_4$ and $TiO_2$ anatase phase were found to increase with increase of calcination temperature.

The XRD observations described above reveal an interesting information about the reactivity of vanadia towards $La_2Ti_2O_7$ and $La_4Ti_9O_{24}$ compounds. The dispersed vanadia reacts preferably with $La_2O_3$ portion of $La_2Ti_2O_7$ and $La_4Ti_9O_{24}$ compounds to form $LaVO_4$, thus, liberating $TiO_2$. The portion of $TiO_2$ released from $La_2Ti_2O_7$ and $La_4Ti_9O_{24}$ compounds appear as the crystalline anatase phase as shown in the following equations:

$$La_2Ti_2O_7 + V_2O_5 \rightarrow 2LaVO_4 + 2TiO_2 \text{ (anatase)} \quad (1)$$

$$La_4Ti_9O_{24} + 2V_2O_5 \rightarrow 4LaVO_4 + 9TiO_2 \text{ (anatase)} \quad (2)$$

It is a well established fact in the literature [2,6,7,32] that a highly dispersed vanadia on $TiO_2$ support accelerates the anatase-into-rutile phase transformation by lowering the activation temperature of this phenomenon, which is normally expected to be 823 K and above in impurity-free $TiO_2$ samples [8]. During this transformation some of the vanadia is normally reduced and gets incorporated into the rutile structure as $V_xTi_{(1-x)}O_2$ (rutile solid solution) [2,6,7,32]. However, in the case of $La_2O_3$-$TiO_2$ mixed oxide support, the reactivity of vanadia towards $La_2Ti_2O_7$ and $La_4Ti_9O_{24}$ compounds appears to be quite different. It

interacts preferably with the lanthana portion of these compounds to form $LaVO_4$ as shown in Eqs. (1) and (2). The liberated titania appears in the form of crystalline anatase phase. This is an interesting observation from this study.

### 3.2. FT-infrared measurements

The FTIR spectra of $La_2O_3$-$TiO_2$ mixed oxide support calcined at 773–1073 K revealed the presence of strong absorption bands between 3400 and 3600 $cm^{-1}$ and at 1625 $cm^{-1}$. In addition, a new peak at 650–830 $cm^{-1}$ was also observed in the case of 1073 K calcined samples. The absorption peaks between 3400 and 3600 $cm^{-1}$, known to be due to the presence of surface hydroxyl groups, were gradually decreased with increase in calcination temperature [33]. The peak at 1625 $cm^{-1}$, due to the deformation vibrations of adsorbed water, was also gradually decreased after calcination at high temperatures [34]. Anatase and rutile phases of titania exhibit strong absorption bands in the region of 850–650 and 800–650 $cm^{-1}$, respectively. A gradual improvement in the region between 850–650 $cm^{-1}$ with increase in calcination temperature was observed suggesting that the titania is gradually transforming from an amorphous to a crystalline anatase phase in line with XRD observations.

The FTIR spectra of various $V_2O_5/La_2O_3$-$TiO_2$ catalysts calcined at different temperatures are recorded in the range of 400–1800 $cm^{-1}$, where those bands due to the $\nu_{V=O}$ are expected to be observed. Normally, the IR spectrum of pure crystalline $V_2O_5$ shows sharp absorption bands at 1020 and another at 820 $cm^{-1}$ due to V=O stretching and V–O–V deformation modes, respectively [35]. The spectrum of 4 wt.% $V_2O_5/La_2O_3$-$TiO_2$ sample calcined at 773 K was identical to that of pure support, in agreement with the XRD observations, where only the anatase phase of $TiO_2$ is noted. With increase in calcination temperature from 773 to 1073 K a gradual change from amorphous to a crystalline anatase formation was noted from FTIR in line with XRD results. A weaker band at around 980 $cm^{-1}$ was noted in the spectrum of the sample calcined at 873 K. On further increase of calcination temperature from 873 to 1073 K the absorption band in the region of 990–960 $cm^{-1}$ was completely diminished, which suggest that the dispersed vanadium oxide is transformed from amorphous $VO_x$ to a different form. However, no absorption band at 1020 $cm^{-1}$ due to V=O stretching mode of crystalline $V_2O_5$ was seen. The disappearance of absorption bands at 990–960 $cm^{-1}$ were also noted in the case of 8 and 12% $V_2O_5/TiO_2$-$La_2O_3$ samples at the calcination of 873 K and above. The formation of crystalline $LaVO_4$ may be the reason for the disappearance of the absorption band at 990–960 $cm^{-1}$ of the dispersed $VO_x$ species [36]. An improvement in the intensity of the absorption band at 830–650 $cm^{-1}$ was also noted when the samples were subjected to calcinations at >773 K. This improvement is more in the case of 12% $V_2O_5/La_2O_3$-$TiO_2$ catalyst. Crystallization of titania anatase was found to be more in the case of 12% catalyst from XRD study. All these observation made from FTIR are in line with the findings of XRD study.

### 3.3. BET surface area and oxygen uptake measurements

The change in BET surface area of sample as a function of calcination temperature is shown in Fig. 6. A considerable decrease in the specific surface area of the catalyst, depending on the calcination temperature and vanadia loading, can be noted from this figure. The decrease in specific surface area with increase in calcination temperature is a general phenomenon and is expected to be due to sintering of the samples at higher temperatures [2,10,15]. Similarly, the decrease in specific surface area with increase of vanadia loading may presumably due to blocking of pores of the support by the dispersed vanadium oxide and also due to the formation of $LaVO_4$ compound. It is an established fact in the literature that a highly dispersed vanadia normally decreases the specific surface area of the support by penetrating in to the pores of the support material [2,10,15,27]. The important point that can be noticed from Fig. 6 is that the decrease in surface area is more in the case of vanadia impregnated catalysts than that of pure support. This observation clearly indicates that the pure lanthana–titania support is more stable when compared to that of vanadia impregnated samples.

Oxygen uptakes at 643 K on pre-reduced $V_2O_5/La_2O_3$-$TiO_2$ catalysts, calcined at different temperatures, as a function of vanadia loading are shown in Fig. 7.

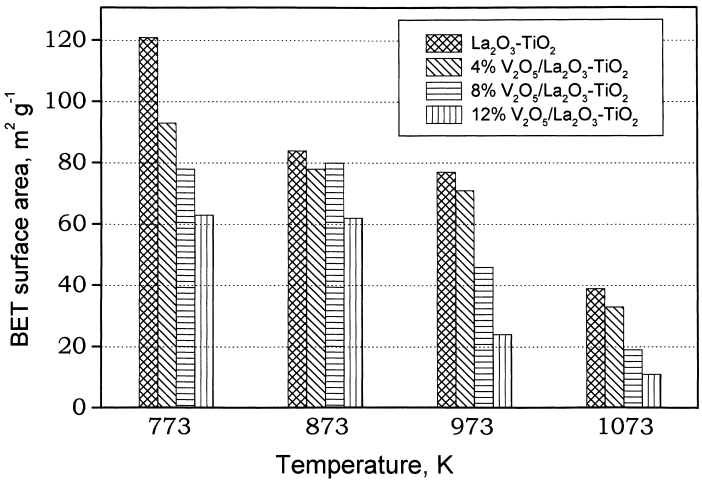


Fig. 6. Effect of calcination temperature on the BET surface area of $La_2O_3$-$TiO_2$ support and various $V_2O_5/La_2O_3$-$TiO_2$ catalysts.

The pure $La_2O_3$-$TiO_2$ support was also found to chemisorb some small amount of $O_2$ (5.2 μmol $g^{-1}$) under the experimental conditions used in this study. Therefore, the contribution of pure support alone was subtracted from the results. As can be noted from Fig. 7, the oxygen uptake increases with increase of vanadia loading. However, the numerical values of $O_2$ uptake varied appreciably and are maximum in the case of catalysts calcined at 773 K and minimum at 1073 K. A large decrease in the $O_2$ uptakes is noted between 873 and 973 K treated samples and such a difference is not found neither between 773 and 873 K nor between 973 and 1073 K treated samples. It can be inferred from these results that the calcination of $V_2O_5/La_2O_3$-$TiO_2$ catalysts at 973 K (the melting point of $V_2O_5$ is 963 K) and above apparently results in the formation of more crystalline $LaVO_4$ compound. The $LaVO_4$ may be formed due to a reaction between $La_2O_3$-$TiO_2$ and the vanadia being leached out from the micro-pores of the support material where

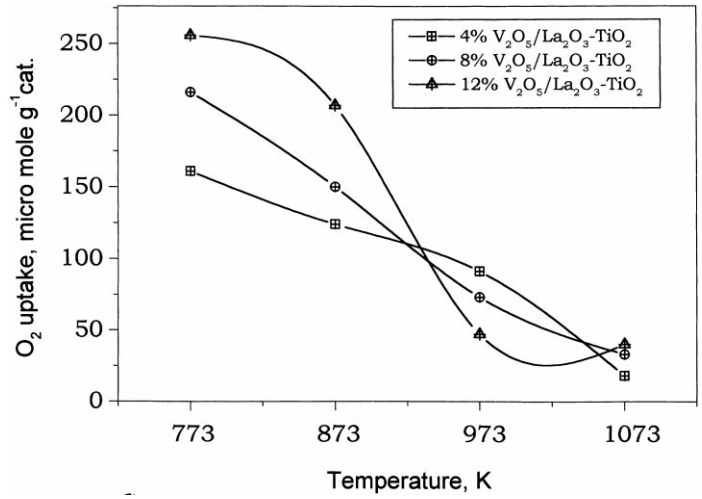


Fig. 7. Effect of calcination temperature on the oxygen uptake capacity of various $V_2O_5/La_2O_3$-$TiO_2$ catalysts. $O_2$ uptake was obtained by a volumetric method at 643 K.

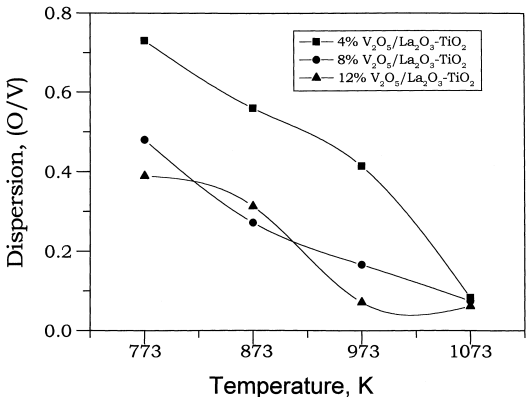


Fig. 8. Effect of calcination temperature on the dispersion of vanadia on $La_2O_3$-$TiO_2$ support. Dispersion was calculated from $O_2$ uptake measurements by assuming $O_2/V_2O_5 = 1$.

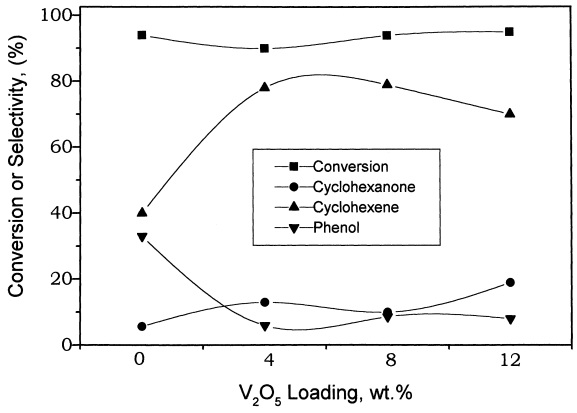


Fig. 9. Conversion of cyclohexanol to different products on $La_2O_3$-$TiO_2$ and $V_2O_5/La_2O_3$-$TiO_2$ samples at 673 K and under normal atmospheric pressure.

it was in a highly dispersed state. A substantial loss in the specific surface area of the catalyst depending on the calcination temperature and vanadia content has been noted (Fig. 6). Thus, calcination of the vanadia containing catalysts brings about a decrease of the specific surface area in all samples studied, being proportional to the temperature of calcination. Recently, Reddy et al. [27] demonstrated that the slope of the plot between oxygen uptake and $V_2O_5$ loading approaches unity at very low loadings. This unity indicates a limiting stoichiometry of $O_2/V_2O_5 = 1$. Using this stoichiometry, Oyama et al. [37] defined dispersion as the ratio of molecular oxygen uptake to $V_2O_5$ content. Fig. 8 represents the dispersions derived from $O_2$ uptake measurements. The apparent dispersion decreases with increase in vanadia loading at a given calcination temperature. This is a general phenomenon observed on any supported catalyst system [10,15,27,38]. Increasing calcination temperature also results in a tremendous decrease in the dispersion of vanadia, especially in the case of catalysts calcined at 1073 K. However, in the case of samples calcined at 773 K the dispersion remains reasonably high at all loadings. Another interesting point to note Fig. 8 is that the vanadia dispersion is reasonably high even at 873 K. The decrease in the dispersion with increase in calcination temperature as well as $V_2O_5$ loading are primarily due to the formation of $LaVO_4$ compound. Thus, $O_2$ uptake results are in line with XRD and FTIR observations.

### 3.4. Conversion of cyclohexanol

For the purpose of better comparison, the steady state activity and selectivity results of cyclohexanol conversion over lanthana–titania and vanadia/lanthana–titania catalysts, at a constant temperature of 673 K and under normal atmospheric pressure, are presented in Fig. 9. As can be noted from this figure, the $La_2O_3$-$TiO_2$ support exhibits more selectivity towards phenol, whereas the $V_2O_5/La_2O_3$-$TiO_2$ catalysts show more selectivity towards cyclohexene. In a recent study, Bezouhanova and Al-Zihari [39] used cyclohexanol conversion as a test reaction to investigate the acid–base properties of different metal oxide catalysts. They reported a direct correlation between Brønsted acid sites and the amount of cyclohexene, the dehydration product, formed. The dehydrogenation product, cyclohexanone, was directly correlated with the basic sites. There is a possibility of formation of coordinatively unsaturated metal cations and oxygen anions on the surface of oxide/binary oxide when obtained from co-precipitation method from the corresponding metal aqueous salt precursors [33]. It is a well-established fact in the literature that exposed coordinatively unsaturated metal cations and oxygen anions on the surface of the catalyst act as Lewis acid and Brønsted base sites [33]. The formation of more amount of phenol over $La_2O_3$-$TiO_2$ than on vanadia impregnated samples may presumably be due to the presence of more surface oxygen anions, which

are expected to be formed in the preparation stage. As the vanadia content increases on the surface of lanthana–titania binary oxide there is a drastic decrease in the selectivity of phenol and a significant improvement in the selectivity of cyclohexene. As per the literature reports [39,40], the $V_2O_5$ is a typical acid, possesses only Brønsted acid sites and produces cyclohexene as the sole product in the reaction of cyclohexanol. The increase in selectivity towards cyclohexene on vanadia impregnated lanthana–titania suggests that vanadia has covered the surface of the carrier. Increasing the content of vanadia on the surface of the support may lead to the formation of octahedral vanadia species having more surface exposed hydroxyl groups [2,41]. It can also be suggested that as the vanadia content increases the exposed coordinately unsaturated sites will be decreased drastically on the surface. It was also noticed that as the reaction temperature increases the selectivity to phenol and cyclohexanone were found to decrease, however, the selectivity towards cyclohexene was increased over all the catalysts investigated. This is primarily due to the fact that as the temperature increases there will be an enhancement in the dehydroxylation of the surface leading to more coordinately unsaturated cations (i.e. Lewis acid sites). More of the surface Lewis acid site population facilitate more interaction of alcohol with the surface leading to more dehydration product, cyclohexene. From this study, it can be inferred that the vanadia impregnated lanthana–titania contains more acidic sites on the surface than that of pure support.

### *3.5. One step synthesis of 2,6-dimethylphenol from methanol and cyclohexanone*

2,6-Dimethylphenol is an important chemical intermediate in the polymer industry for engineering plastics [42]. The commercial synthetic method is based on a liquid phase process, where phenol is methylated with methanol using an alumina catalyst. However, this process not only requires high pressure and temperature, but also produces wide range of byproducts, including various isomers of xylenol [43]. In fact, there are several advantages like continuous production, simplified product recovery, catalyst regenerability, etc. for carrying out this reaction in the vapor phase from cyclohexanone and methanol. In a recent publication, Wang et al. [44] reported the synthesis of 2,6-dimethylphenol from methanol and cyclohexanone over vanadia/titania catalyst. However, the conversion and product selectivities reported are limited on this catalyst. The mixed oxide supports have attracted much attention recently because of their better performance than their constituent single oxides for various reactions [45–47]. Therefore, this particular reaction was selected in the present investigation to study the catalytic properties of $La_2O_3$-$TiO_2$ and $V_2O_5/La_2O_3$-$TiO_2$ catalysts.

The activity and selectivity for the single step synthesis of 2,6-dimethylphenol was investigated between 573 and 698 K. The activity and selectivity trends on various catalysts followed the same pattern with temperature. In general, an increase in the conversion with an increase in temperature was observed. The formation of some additional side products with traces of CO and $CO_2$ were also occasionally noted at higher temperatures. The change in conversion as a function of contact time at a fixed temperature of 673 K was also studied on various catalysts. A decrease in the conversion of cyclohexanone during the initial reaction period was observed for all the catalysts used, but stable activity was obtained within a few hours. The conversion and selectivity are calculated on cyclohexanone basis and almost all the excess methanol was recovered after the reaction. The conversion and selectivity results as a function of temperature on the $La_2O_3$-$TiO_2$ support and the 12% $V_2O_5/TiO_2$-$La_2O_3$ catalyst are presented in Figs. 10 and 11, respectively. As can be noted from these figures, the conversion of cyclohexanone was found to increase as the reaction temperature increases. On the $La_2O_3$-$TiO_2$ support, at low reaction temperatures the formation of 1-methoxycyclohexene, methyl formate, and dimethyl ether in large amounts was noted in addition to small amounts of 2-methylcyclohexanone, 2,6-dimethylcyclohexanone, and 2,6-dimethylphenol. At 648 K and above temperatures more selectivity towards 2-methylcyclohexanone and 2,6-dimethylcyclohexanone and a less selectivity towards 2,6-dimethylphenol can be seen. However, at all these temperatures the formation of methyl formate, dimethyl ether, and $CO_x$ in small quantities was noted. Upon impregnating the support with vanadia a major change in the product distribution was noticed. In the case of vanadia impregnated catalysts, the main products observed were 2,6-dimethylphenol,

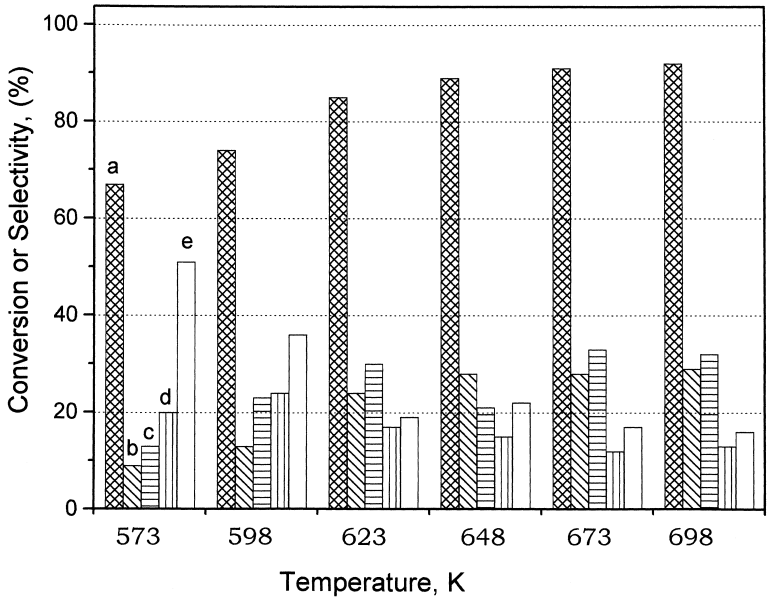


Fig. 10. Activity and selectivity results of one step synthesis of 2,6-dimethylphenol from cyclohexanone and methanol over $La_2O_3$-$TiO_2$ support at different temperatures: (a) conversion; (b) selectivity to 2,6-dimethylphenol; (c) 2,6-dimethylcyclohexanone; (d) 2-methylcyclohexanone; (e) 1-methoxycyclohexene.

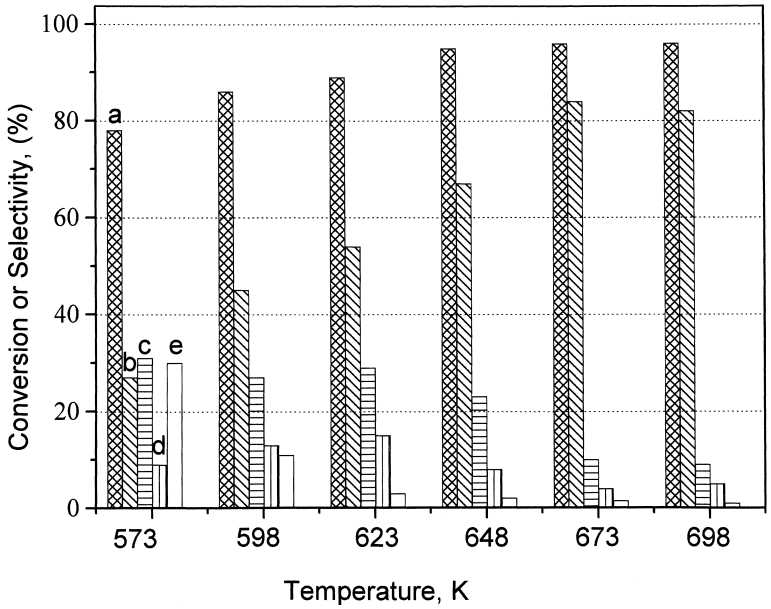


Fig. 11. Activity and selectivity results of one step synthesis of 2,6-dimethylphenol from cyclohexanone and methanol over 12 wt.% $V_2O_5/La_2O_3$-$TiO_2$ catalyst at different temperatures: symbols as in Fig. 10.

Table 1
Catalytic and physicochemical properties of various mixed oxide based vanadium oxide catalysts

| Catalyst[a] | Conversion (%) | 2,6-DMP selectivity (%) | 2,6-DMP yield | BET SA ($m^2\,g^{-1}$) | $O_2$ uptake ($\mu mol\,g^{-1}$) | Cyclohexanone TOF ($\times\ 10^{-3}$) | | Composition[d] (molar ratio) |
|---|---|---|---|---|---|---|---|---|
| $14\%V_2O_5/TiO_2$-$Al_2O_3$ | 87 | 54 | 47 | 108 | 319 | 0.389[b] | 0.940[c] | 1:1 |
| $14\%V_2O_5/TiO_2$-$ZrO_2$ | 76 | 56 | 43 | 126 | 233 | 0.396[b] | 1.123[c] | 1:1 |
| $20\%V_2O_5/TiO_2$-$SiO_2$ | 92 | 64 | 59 | 151 | 903 | 0.286[b] | 0.359[c] | 1:1 |
| $12\%V_2O_5/In_2O_3$-$TiO_2$ | 64 | 19 | 12 | 61 | 911 | 0.332[b] | 0.240[c] | 1:13 |
| $12\%V_2O_5/Ga_2O_3$-$TiO_2$ | 90 | 65 | 58 | 51 | 532 | 0.931[b] | 0.671[c] | 1:5 |
| $4\%V_2O_5/La_2O_3$-$TiO_2$ | 92 | 48 | 44 | 93 | 161 | 2.830[b] | 5.450[c] | 1:5 |
| $8\%V_2O_5/La_2O_3$-$TiO_2$ | 93 | 55 | 51 | 78 | 216 | 1.410[b] | 2.870[c] | 1:5 |
| $12\%V_2O_5/La_2O_3$-$TiO_2$ | 96 | 84 | 81 | 63 | 256 | 0.990[b] | 2.550[c] | 1:5 |

[a] $V_2O_5$ content in wt.%.
[b] Number of molecules of cyclohexanone converted per vanadium atom per second.
[c] Number of molecules of cyclohexanone converted per active oxygen atom per second.
[d] Support composition.

2,6-dimethylcyclohexanone, 2-methylcyclohexanone and 1-methoxycyclohexene, respectively. In the case of vanadia/lanthana–titania catalysts, maximum selectivity towards 2,6-dimethylphenol was noted at 648 K and above temperatures (Fig. 11). Similar results were also noted on 4 and 8% catalysts. In general, the selectivity of 2,6-dimethylphenol increased with increase in temperature and at the same time the selectivity towards 2,6-dimethylcyclohexanone, 2-methylcyclohexanone and 1-methoxycyclohexene decreased drastically. An improvement in the conversion and selectivity was observed upon increasing the loading of vanadium oxide on the support. The 12 wt.% $V_2O_5/La_2O_3$-$TiO_2$ catalyst exhibited more conversion and selectivity.

For the purpose of comparison, the activity and selectivity trends over various vanadia-containing catalysts were obtained and shown in Table 1. The investigated $TiO_2$-$SiO_2$, $TiO_2$-$Al_2O_3$, $TiO_2$-$ZrO_2$, $La_2O_3$-$TiO_2$, $Ga_2O_3$-$TiO_2$, and $In_2O_3$-$TiO_2$ mixed oxides are known to possess different solid acid–base properties. As can be noted from Table 1, the cyclohexanone TOF is highly dependent on the vanadia loading. Among various metal oxides tested the 12% $V_2O_5/La_2O_3$-$TiO_2$ exhibited favorable characteristics for the single step synthesis of 2,6-dimethylphenol and provided maximum yield reported so far.

The formation of 2,6-dimethylphenol from methanol and cyclohexanone is shown schematically in Eq. (3). The product distribution observed gives an impression that this reaction proceeds in a different manner from that of normal methylation of aromatic compounds. In general, in the alkylation of substituted aromatic compounds, one can occasionally observe a mixture of *ortho*-, *para*-, or *meta*-substituted products depending on the type of precursors, reaction conditions and the catalyst used. However, in the present case *ortho*-substituted phenol and/or cyclohexanone are exclusively formed from methanol and cyclohexanone mixtures. The non-formation of *meta*- or *para*-substituted products and the selective formation of 1-methoxycyclohexene, 2-methylcyclohexanone, 2,6-dimethylcyclohexanone, and 2,6-dimethylphenol suggest that the reaction may proceed as shown in Scheme 1.

As shown in Scheme 1, in the first step of reaction the cyclohexanone condenses with a methanol molecule, in its another isomeric form enol, and produces 1-methoxycyclohexene, which was obtained as one of the side products. Thus, produced 1-methoxycyclohexene over isomerization produces 2-methylcyclohexanone. Thus, formed 2-methylcyclohexanone by condensing with another molecule of methanol produces 2,6-dimethylcyclohexanone as

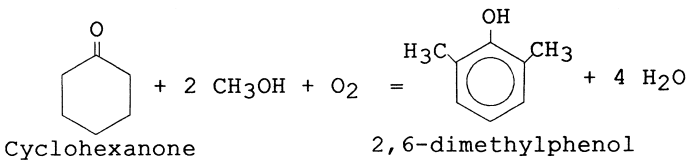


(3)

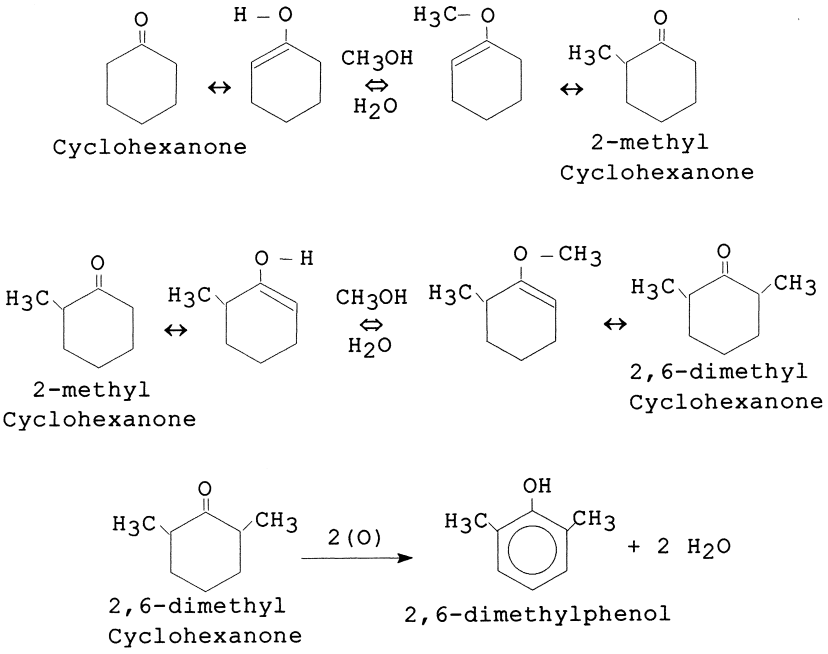


Scheme 1.

shown in the Scheme 1. It is a well-established fact in the literature that the transition metal oxides, such as $V_2O_5$, $MoO_3$, etc. are very active for the oxidative dehydrogenation of organic molecules [48,49]. Thus, formed 2,6-dimethylcyclohexanone by oxidative dehydrogenation probably produces the 2,6-dimethylphenol. However, further studies are highly essential to establish the mechanism of this complex reaction.

Under dehydrated conditions, surface vanadia species possesses terminal V=O groups and polymeric functionalities associated with isolated and polymerized species on the support surface [50]. The molecular structures of the surface $VO_x$ species are known to consist of a terminal V=O bond and three bridging V–O–Support bonds in the case of isolated species, and a terminal V=O bond with one bridging V–O–S and two bridging V–O–V bonds for the polymerized species [51]. These structures are highly dependent on the nature of the support material and on the amount of vanadium oxide deposited. It is known that the concentration of polymerized surface functionality increases with vanadium oxide coverage on the support surface. Hence, as the vanadium oxide loading increases up to monolayer coverage on the surface of the support material, along with V=O bonds, the V–O–S bonds also increases. However, at above monolayer coverages the increase of vanadia loading increases only the V=O and V–O–V bonds and not the V–O–S bonds. Reddy et al. [27,28] have recently observed that the yield of isobutyraldehyde increases up to the monolayer coverage and declines slightly beyond the monolayer loading. However, in the present case the TOF of cyclohexanone conversion decreases with increase of vanadia loading. A comparison of activity trends with vanadia loading clearly indicates that the V–O–S bonds may be the probable active participants in the synthesis of 2,6-dimethylphenol from methanol and cyclohexanone. Change of specific mixed oxide support does have a significant effect on the cyclohexanone or 2,6-dimethylphenol TOFs (Table 1). This observation further supports that the bridging V–O–Support bonds may be involved in the critical kinetic steps of the cyclohexanone conversion or 2,6-dimethylphenol formation.

Comparison of cyclohexanone conversion or 2,6-dimethylphenol formation with other reactions over the same supported vanadium oxide catalysts

can provide additional understanding on the fundamental aspects of this reaction. The selective oxidation of 4-methylanisole to anisaldehyde over supported vanadia catalysts was found to depend on the acid–base properties of the support oxide apart from vanadia surface coverages [52]. Recently, Deo and Wachs [53] have studied the methanol oxidation on a number of supported vanadium oxide catalysts. They found that the activity of the alcohol oxidation correlates with the extent of reduction and strength of V=O and V–O–S bonds. However, it is difficult to establish such a direct correlation in the present study because of the complexity of the reaction involved.

## 4. Conclusions

The following conclusions can be drawn from this study: (1) The lanthana–titania binary oxide is an interesting and promising support material for the dispersion of vanadium oxide. (2) The co-precipitated $La_2O_3$-$TiO_2$ mixed oxide when calcined at 773 K is in X-ray amorphous state and exhibits reasonably high specific surface area. The amorphous $La_2O_3$-$TiO_2$ gets converted into crystalline $La_2Ti_2O_7$ and $La_4Ti_9O_{24}$ compounds at 873 and 1073 K, respectively. (3) The $La_2O_3$-$TiO_2$ mixed oxide also accommodates a monolayer equivalent of $V_2O_5$ (12 wt.%) in a highly dispersed state on its surface. Further, the $V_2O_5/La_2O_3$-$TiO_2$ catalyst is thermally stable up to 873 K calcination temperature. When subjected to thermal treatments beyond 873 K, the dispersed vanadium oxide selectively interacts with $La_2O_3$ portion of the $La_2O_3$-$TiO_2$ mixed oxide and readily forms $LaVO_4$ compound with the release of $TiO_2$. The liberated $TiO_2$ appears in the form of anatase phase. (4) Among various catalysts investigated, the $V_2O_5/La_2O_3$-$TiO_2$ combination is a promising system for the one step synthesis of 2,6-dimethylphenol from methanol and cyclohexanone mixtures. In particular, the 12 wt.% $V_2O_5/La_2O_3$-$TiO_2$ catalyst provided a maximum yield of 2,6-dimethylphenol.

Finally, further studies are highly essential in order to understand the microscopic mechanism of this reaction and the inter relationships between the acid–base and redox characteristics of the catalyst and their catalytic properties.

## Acknowledgements

Ibram Ganesh thanks the University Grants Commission, New Delhi for the award of a senior research fellowship.

## References

[1] D.J. Hucknall, Selective Oxidation of Hydrocarbons, Academic Press, London, 1974.
[2] G.C. Bond, S.F. Tahir, Appl. Catal. 71 (1991) 1 and references therein.
[3] G. Deo, I.E. Wachs, J. Haber, Crit. Rev. Sci. Eng. 19 (1994) 141.
[4] I.M. Pearson, H. Ryu, W.C. Wong, K. Nobe, Ind. Eng. Chem. Prod. Res. Dev. 22 (1983) 381.
[5] A. Baiker, P. Dellenmeir, M. Glinski, A. Reller, Appl. Catal. 35 (1989) 351.
[6] R. Kozlowski, R.F. Pettifer, J.M. Thomas, J. Phys. Chem. 87 (1983) 5176.
[7] F. Roozeboom, M.C. Mittlemeijer-Hazeleger, J.A. Moulin, J. Medema, V.H.J. de Beer, P.J. Gellings, J. Phys. Chem. 84 (1980) 2783.
[8] S.R. Yoganarasimhan, C.N.R. Rao, Trans. Faraday Soc. 58 (1962) 1579.
[9] K.-N.P. Kumar, Appl. Catal. A: Gen. 119 (1994) 163.
[10] B.M. Reddy, M.V. Kumar, E.P. Reddy, S. Mehdi, Catal. Lett. 36 (1996) 187.
[11] H.K. Matralis, M. Ciardelli, M. Ruwet, P. Grange, J. Catal. 157 (1995) 368.
[12] K. Jiratova, O. Solcova, H. Snajdaufova, L. Moravkova, H. Zahradnikova, V. Ponec, M. Shamanska, H.U. Blaser, Stud. Surf. Sci. Catal. 75 (1993) 1235.
[13] K.-N.P. Kumar, K. Keizer, A.J. Burggraaf, J. Mater. Sci. Lett. 13 (1994) 59.
[14] G. Olivery, G. Ramis, G. Busca, V.S. Escribano, J. Mater. Chem. 3 (1993) 1239.
[15] B.M. Reddy, S. Mehdi, E.P. Reddy, Catal. Lett. 20 (1993) 317.
[16] B.M. Reddy, B. Manohar, S. Mehdi, J. Solid State Chem. 96 (1992) 233.
[17] C.A. Le Duc, J.M. Campbell, J.A. Rossin, Ind. Eng. Chem. Res. 35 (1996) 2473.
[18] Z. Kalenik, E.E. Wolf, Stud. Surf. Sci. Catal. 61 (1991) 97.
[19] G.S. Lane, Z. Kalenik, E.E. Wolf, Appl. Catal. 53 (1989) 183.
[20] Z. Bocun, W. Ren, Zhongguo Xitu Xuebao (China), 9(1) (1991) 40 CA Vol. 115: 264300k.
[21] K.-N.P. Kumar, K. Keizer, A.J. Burggraaf, J. Mater. Chem. 3 (1993) 1412.
[22] U. Trudinger, G. Muller, K.K. Unger, J. Cromatogr. 35 (1990) 111.
[23] S.-J. Huang, A.B. Walters, M.A. Vannice, J. Catal. 173 (1998) 229.
[24] H. Borchert, M. Baerns, J. Catal. 168 (1997) 315.

[25] A. Slagtern, Y. Schuurman, C. Leclercq, X. Verykios, C. Mirodatos, J. Catal. 172 (1997) 118.
[26] H.P. Klug, L.E. Alexander, X-ray Diffraction Procedures for Polycrystalline and Amorphous Materials, 2nd Edition, Wiley, New York, 1974.
[27] B.M. Reddy, B. Manohar, E.P. Reddy, Langmuir 9 (1993) 1781.
[28] B.M. Reddy, E.P. Reddy, I. Ganesh, Res. Chem. Intermed. 23 (1997) 703.
[29] F. Roozeboom, T. Franson, P. Mars, P.J. Gellings, Z. Anorg. Allg. Chem. 449 (1979) 25.
[30] R. Gopalan, Y.S. Lin, Ind. Eng. Chem. Res. 34 (1995) 1189.
[31] T.F. Limar, N.G. Kisela, Neorg. Mater. 10 (10) (1974) 1826 (Russia), CA No. 82: 77618h.
[32] A. Vejux, P. Courtine, J. Solid State Chem. 23 (1978) 93.
[33] H.H. Kung, Stud. Surf. Sci. Catal (Transition Metal Oxides, Surface Chemistry and Catalysis) 45 (1988) 57.
[34] A. Jentys, G. Warecka, M. Derewinski, J.A. Lercher, J. Phys. Chem. 93 (1989) 4837.
[35] G.C. Bond, A.J. Sarkany, G.D. Parfitt, J. Catal. 57 (1979) 476.
[36] Y. Nakagawa, O. Ono, H. Miyata, Y. Kubokawa, J. Chem. Soc., Faraday Trans. 79 (1983) 2929.
[37] S.T. Oyama, G.T. Went, A.T. Bell, G.A. Somarjai, J. Phys. Chem. 93 (1989) 6786.
[38] B.M. Reddy, K. Narsimha, P.K. Rao, V.M. Mastikhin, J. Catal. 118 (1989) 22.
[39] C.P. Bezouhanova, M.A. Al-Zihari, Catal. Lett. 11 (1991) 245.
[40] A. Auroux, A. Gervasini, J. Phys. Chem. 94 (1990) 6371.
[41] G. Deo, I.E. Wachs, J. Catal. 129 (1991) 307 .
[42] J.M. Margolis, Engineering Thermoplastics: Properties and Applications, Marcel Dekker, New York, 1985.
[43] K. Weissermel, H.-J. Arpe, Industrielle Organische Chemie, Verlag Chemie, GmbH, Weium, Germany, 1976.
[44] F.L. Wang, L. Yu, W.S. Lee, W.F. Wang, J. Chem. Soc., Chem. Commun. (1994) 811.
[45] I. Wang, R.C. Chang, J. Catal. 107 (1987) 195.
[46] B.E. Hand, M. Maciejewski, A. Baiker, J. Catal. 134 (1992) 75.
[47] B.M. Reddy, B. Chowdhury, J. Catal. 179 (1998) 413.
[48] B. Manohar, I. Ganesh, B.M. Reddy, J. Mol. Catal. A: Gen. 129 (1998) L5.
[49] A. Lisovski, C. Ahroni, Catal. Rev. Sci. Eng. 36 (1994) 25.
[50] N. Das, H. Eckert, H. Hu, I.E. Wachs, F. Feher, J. Phys. Chem. 97 (1993) 8240.
[51] G. Busca, G. Centi, F. Trifiro, Appl. Catal. 25 (1986) 265.
[52] B.M. Reddy, I. Ganesh, B. Chowdhury, Chem. Lett. (1997) 1145.
[53] G. Deo, I.E. Wachs, J. Catal. 156 (1994) 323.